Density Functional Theory Study of Structural and Electronic Properties of γ'-Ni₃Al and γ''-Ni₃Nb

D. K. Gorai[*]**, T. K. Kundu**

Department of Metallurgical and Materials Engineering,
Indian Institute of Technology Kharagpur, Kharagpur, WB, India-721302

[*]E-mail: deepakrai0134@gmail.com

Abstract: In the present paper, the structural and electronic properties of ordered face-centered cubic (L1₂) γ'-Ni₃Al and body-centered tetragonal (D0₂₂) γ''-Ni₃Nb are investigated by density functional theory calculation within projector augmented wave (PAW) potentials. The structures are optimized for both the phases and the results are found in good agreement with the experimental and theoretical data. In the geometrical optimization, all the forces on each atom are converged to less than 10^3 eV/Å, and the total energy less than 10^{-6} eV/atom. The Methfessel–Paxton smearing width of 0.2 eV is used here. The formation energy of γ'-Ni₃Al and γ''-Ni₃Nb phases are calculated and the values are found to be -40.67 kJ/mol and -27.55 kJ/mol respectively. The bonding character is analyzed based on the density of states (DOS).
**Keywords: DFT, γ'- phase, γ''- phase, DOS**

1. Introduction

Nickel-based superalloys are extensively used for high-temperature components such as gas turbine disks and aero engine[1]. ALLVAC 718+ is a nickel-based superalloy which can be used as a disc material for high-pressure turbine discs and compressor. This alloy has high-temperature stability and offers a full 55°C temperature advantage over alloy 718 [2].The principal strengthening phases in ALLVAC 718+ are γ'-Ni₃Al and γ''-Ni₃Nb. Hence, it is very important to calculate the structural, mechanical and electronic properties of γ'-Ni₃Al phase and γ''-Ni₃Nb phase.The first-principle density functional theory is extensively used to calculate the structural, mechanical and electronic properties of inter-metallic compounds. A number of studies, particularly on mechanical properties, is carried out on Ni₃Al[3][4]. Yasuda et al. [3] calculated the three elastic stiffness constants of different inter-metallic compounds such as Ni₃Al, Ni₃Mn, Ni₃Fe, Ni₃Si etc.. The structure, mechanical and magnetic properties of Ni₃Al, Ni₃In and Ni₃Ga was investigated by Boucetta et al. [4] using first principle and experimental studies. Yu et al. [5] studied the effects of pressure on elastic properties and thermal conductivity of γ''-Ni₃Nb phase. Cozar and Pineau [6] used X-ray diffraction to measure the lattice parameter of γ''-Ni₃Nb phase. However, there are few reports on the relationship between γ'-Ni₃Al phase and γ''-Ni₃Nb phase.

In this paper, we have used first-principle calculation within the framework of density functional theory (DFT) [7] to calculate the structural and electronic properties of γ'-Ni₃Al and **γ''-**Ni₃Nb phases. The bonding character is analyzed based on the total density of states (TDOSs) and partial density of states (PDOSs).

2. Materials and methods

In ALLVAC 718 plus, γ'-Ni₃Al and γ''-Ni₃Nb phases are the primary strengtheners by chemical and coherency strain hardening. The γ'-Ni₃Al belongs to ordered face-centered cubic (FCC) L1₂ crystal structure whose space group is Pm-3m (S.G. No 221). In the unit cell, there is one formula unit (Z=1) as shown in Figure 1(a). The γ''-Ni₃Nb belongs to ordered body-centered tetragonal (BCT) D0₂₂ crystal structure whose space group is 14/mmm (S.G. No 139). In the unit cell, there is two formula units (Z=2) as shown in Figure 1(b).

<div align="center">(a)   (b)</div>
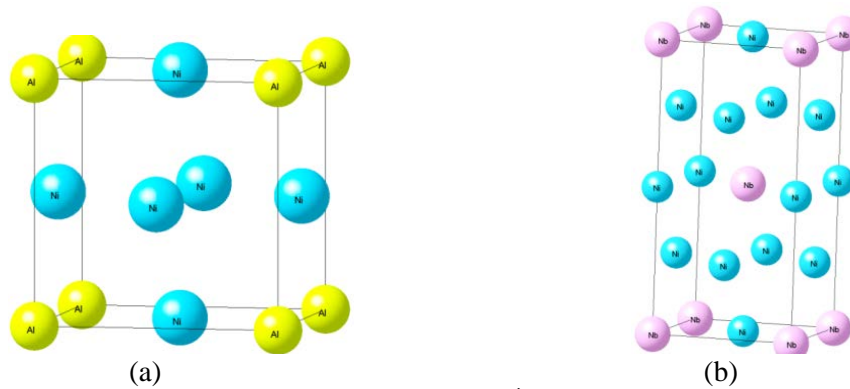
Figure.1: The crystal structure of (a) γ'-Ni$_3$Al and (b) γ''-Ni$_3$Nb

In present work, the density functional theory implemented in the Vienna ab initio Simulation Package (VASP)[8] is used for the calculation. The projected augmented wave method (PAW) [9] is used to describe the ion-electron interactions. The structural calculations are performed independently using two separate approximation, (a) local density approximation (LDA) by Predew and Zunger[10] and (b) generalized gradient approximation of Perdew, Becke and Ernzerhof(GGA-PBE) [11] description of the exchange-correlation functional. Valence-electron configuration for pseudo-atoms are Ni-3d^{8}4s^2, Al-3s^{2}3p^1, and Nb-4d^{4}5s^1.

In the calculation of γ'-Ni$_3$Al, initially the structure is optimized for different values of k-mesh as given in Table 1. From the Table 1, it is observed that the12x12x12 k-mesh optimized the structure with a minimum energy of -2111.55 kJ/mol. Therefore, the k-mesh 12x12x12 is used for the Brillouin Zone (BZ) sampling with a plane wave cut-off energy of 500 eV for both LDA and GGA method. Similarly, for γ''-Ni$_3$Nb phase the structure is optimized for different values of k-mesh as given in Table 2. From the Table 2, it is observed that the 10x10x5 k-mesh optimized the structure with a minimum energy of -2687.45 kJ/mol and therefore, the k-mesh 10x10x5 is used for BZ sampling with a plane wave cut-off energy of 500 eV for both LDA and GGA method. In the geometrical optimization of both the phases, all the forces on each atom are converged to less than 10^{-3} eV/Å, and the total energy less than 10^{-6} eV/atom. The atomic arrangements are relaxed using the Methfessel–Paxton method [12] with a smearing width of 0.2 eV. The Brillouin-zone integration is performed by the tetrahedron method with Blöchl corrections [13].

Table 1.. Optimized structural parameter of γ'-Ni$_3$Al for different values of k-mesh

k-mesh	a=b=c(Å)	Volume (Å^3)	Density(Kg/m^3 x 10^3)	Energy (kJ/mol)
16x16x16	3.57	45.38	7.43	-2111.55
12x12x12	3.57	45.37	7.43	-2111.55
11x11x11	3.57	45.37	7.43	-2111.55
10x10x10	3.57	45.38	7.43	-2111.47
8x8x8	3.57	45.38	7.43	-2111.33

Table 2. Optimized structural parameter of γ''-Ni$_3$Nb for different values of k-mesh

k-mesh	a=b (Å)	c (Å)	Volume(Å^3)	Density(Kg/m^3 x 10^3)	Energy (kJ/mol)
12x12x6	3.65	7.46	99.14	9.01	-2686.37
10x10x5	3.64	7.49	99.19	9.01	-2687.45
8x8x4	3.64	7.49	99.18	9.01	-2687.44
6x6x3	3.65	7.47	99.16	9.01	-2686.15

3. Result and Discussion

3.1 Structure Properties and stability

The total energy is calculated as a function of cell volume and fitted by the Brich-Murnaghan equation of states (EOS) [14] to find the equilibrium lattice constants. The optimized equilibrium cell volume and lattice parameters a_0 of Ni_3Al phase and a_0 and c_0 of Ni_3Nb phase is calculated. The theoretical and experimental results from the references[15][16][17][18][19][20], as well as the results calculated in the present work by both GGA and LDA methods, are given in Table 3 and Table 4 for Ni_3Al and Ni_3Nb respectively. It is found that for Ni_3Al, the value calculated by GGA method is in accordance with other calculations values [15][16] and as well as the experimental value [17][18]. The value calculated by LDA method is smaller than the experimental value. For the Ni_3Nb phase, the values of lattice constants a_0 and c_0 are respectively 0.55% and 0.78% higher than the experimental values, while the values of lattice constants a_0 and c_0 calculated by LDA method are respectively 1.74% and 0.78% smaller than the experimental values. Apart from this, the value of a_0/c_0 calculated by LDA method is not closer to the experimental value while the value of a_0/c_0 calculated by GGA method is closer to the experimental value. Hence, GGA method is used here for the subsequent calculation of stability of both Ni_3Al and Ni_3Nb phase. The LDA values are just used here as the reference for succeeding calculations.

Table 3: The calculated and experimental values of lattice constant (a_0), equilibrium cell volume (V_0) and bulk modulus (B_0) at 0 GPa of Ni_3Al phase

$a_0(Å)$	$V_0(Å)^3$	$B_0(GPa)$
3.57	45.37	-
3.48	42.17	-
3.57 [15]	45.65	182.0 [16]
3.57 [17]	45.58	179.3 [18]

Table 4: The calculated and experimental values of lattice constants (a_0,c_0), equilibrium cell volume (V_0) and bulk modulus (B_0) at 0 GPa of Ni_3Nb phase

$a_0(Å)$	$c_0(Å)$	c_0/a_0	$V_0(Å)^3$	$B_0(GPa)$	References
3.64	7.46	2.05	99.16	-	Present work (GGA-PBE)
3.56	7.75	2.06	92.57	-	Present work (LDA)
3.65	7.51	2.06	99.99	208.6	[19]
3.64	7.48	2.05	99.32	208	[20]

Generally, the formation enthalpy [21] is used as a measure of the stability of a phase. A negative formation enthalpy results in an exothermic process and a stable phase, while positive value implies in an unstable phase and endothermic process. In the present work, the following formula is used to calculate the formation enthalpy:

$$\Delta H(Ni_xAl_yNb_z) = \frac{E_{total} \left(Ni_xAl_yNb_z\right) - xE_{solid} (Ni) - yE_{solid} (Al) - zE_{solid} (Nb)}{(x+y+z)} \tag{1}$$

where, x, y, and z are the mole fraction of Ni, Al and Nb in the alloy. $E_{total} \left(Ni_xAl_yNb_z\right)$, $E_{solid} (Ni), E_{solid} (Al)$ and $E_{solid} (Nb)$ are respectively the total energy of a $Ni_xAl_yNb_z$ alloy that relaxed to their equilibrium state and the total energies of elements Ni, Al and Nb (per atom), which are obtained from the first principle calculations. In case of Ni_3Al phase, the value of z is zero while, the value of y is zero in the case of Ni_3Nb phase. The total energies, symmetry group and the atomic radius of pure elements Ni, Al and Nb (per atom) in their ground state is given in Table 5. The values

of total energies and formation enthalpies of Ni_3Al and Ni_3Nb phases are given in the Table 6. The results are in good harmony with the available theoretical result [20][23]. The negative value of formation enthalpy suggests an exothermic process and the thermodynamical stability of both the phases. It is noted, from the Table 6 that the value of formation enthalpy of Ni_3Al phase is -40.669 kJ/atom, which is smaller than the value of formation enthalpy -27.547 kJ/atom of Ni_3Nb phase. Hence it shows that the Ni_3Al phase with ordered face-centered cubic (FCC) $L1_2$ crystal structure is thermodynamically more stable than the Ni_3Nb phase with ordered body-centered tetragonal (BCT) $D0_{22}$ crystal structure. The less negative formation enthalpy of Ni_3Nb phase also indicates that it is thermodynamically not very strong. This is in good harmony with the experimental investigation which indicates that metastable γ"-Ni_3Nb phase is changed into more stable delta (δ- Ni_3Nb) phase below 900^oC for a long time [24].

Table 5: Lattice constants, symmetry group, atomic radius, and total energies of pure
elements per atom in their ground state.

Elements	a_0(Å)	Symmetry group	Atomic radius (Å)	Energy (kJ/mol)	Reference
Ni	3.52	FM3M	1.62	-529.33	This work
	3.52	-	-	-527.72	[22]
Al	4.04	FM3M	1.82	-360.96	This work
	4.05	-	-	-356.69	[22]
Nb	3.31	IM3M	2.08	-988.04	This work

Table 6: Calculated total energy (E_{tot}) and formation enthalpy (ΔH) of Ni_3Nb and Ni_3Al phases.

| Ni_3Nb	E_{tot}(kJ/mol)	ΔH (kJ/mol)	Ni_3Al	E_{tot}(kJ/mol)	ΔH(kJ/mol)
GGA	-2687.19	-27.55	GGA	-2111.64	-40.67
LDA	-3115.30	-134.79	LDA	-4068.51	-135.88
Ref. [20]	-	-29.72	Ref.[23]	-	-43.98

3.2 Electronic Properties

Both GGA and LDA methods are used to calculate the total density of states (TDOSs) and partial density of states (PDOSs) of Ni_3Al phase and Ni_3Nb phase, at zero pressure to study underlying mechanism of mechanical properties and structural stability from the nature of the chemical bonding. It is found that the result calculated by both methods display the similar patterns. Hence, for the ease, we have just given the results calculated by the GGA method.

In Figure 2(a) and Figure 2(b), the total density of states and partial density of states of both the phases have been given. It is found that the value of the density of states for both the phases, at Fermi energy is non-zero, which reveals that both the phases have metallic characteristics. It is shown in Figure 2(a), that the Ni *3d* states and Al *3p* states control the contributions to the total density of states and also there exists a little difference between the spin-up and spin-down states, which indicates a weak magnetism of Ni_3Al[25]. It is found that there is no distinction between the spin-up and spin-down in Ni_3Nb phase (Figure 2(b)), hence there is no magnetism in this phase. Next, from the Figure 3(a) it is found that there is no overlapping in Al *3p* and Ni *4d*, so there is no covalent interaction in Ni_3Al, but from Figure 3(b), it is clear that there is a complete overlapping between Ni *3d* and Nb*4d* states, which indicates there exists covalent interaction in Ni_3Nb phase.
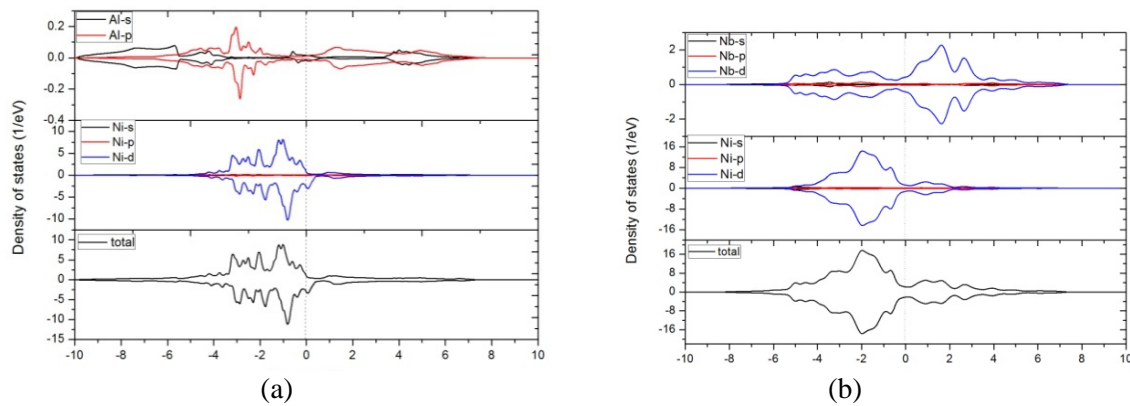
Figure 2: Total and partial density of states (a) Ni$_3$Al phase and (b) Ni$_3$Nb phase
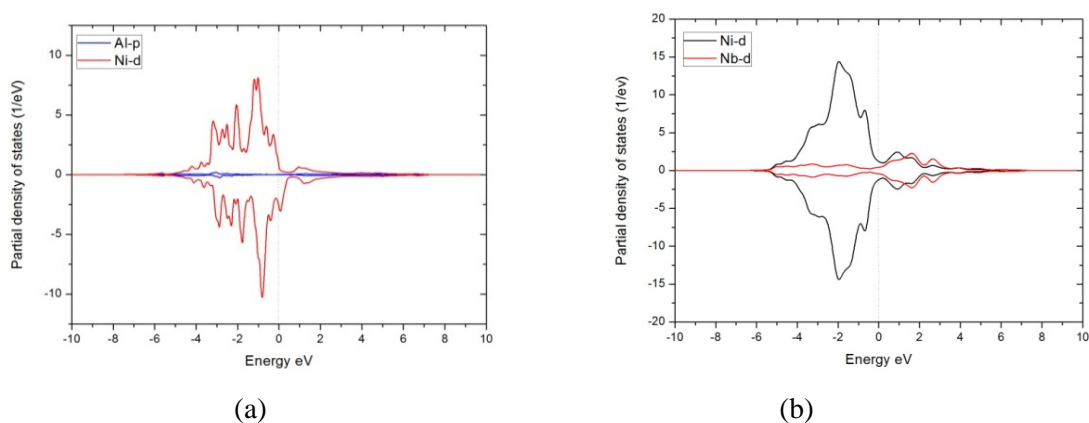
Figure 3: Partial density of states (a) Ni$_3$Al phase and (b) Ni$_3$Nb phase

4. Conclusion

In the present work, we have calculated the structural and electronic properties of $\gamma^{'}$-Ni$_3$Al and $\gamma^{''}$-Ni$_3$Nb using first principle density functional theory calculation at 0 GPa pressure. The calculated lattice constants are in good harmony with the experimental and theoretical results. The negative value of formation energy points out that both phases are thermodynamically stable. The more negative value of formation energy in the case of $\gamma^{'}$-Ni$_3$Al phase indicates that $\gamma^{'}$-Ni$_3$Al is thermodynamically more strong than $\gamma^{''}$-Ni$_3$Nb, which is in good accordance with the experimental investigation which suggests that metastable $\gamma^{''}$-Ni$_3$Nb phase is changed into more stable delta (δ- Ni$_3$Nb) phase below 900°C for a long time. The density of states reveals that there exists a covalent interaction in $\gamma^{''}$-Ni$_3$Nb.

References:

[1] Zhang H Y, Zhang S H, Cheng M, and Li Z X 2010 *Mater. Charact*. **61** pp. 49–53.
[2] Kennedy R L, Cao W D, Bayha T D and Jeniski R 2004 *Niobium for High Temperature Applications*, ed. by Young-Won Kim and Tadeu Carneiro TMS pp. 11-21.
[3] Yasuda H, Takasugi T, Koiwa M 1992 *ActaMetall Mater* **40** 381.
[4] Boucetta S, Chihi T, Ghebouli B and Fatmi M 2010 *Mater Sci Poland* **28** 347.
[5] Lin Y C, Luo S C, Chen M S and He D G 2016 *Journal of Alloys and Compounds* **688** pp

285- 293.

[6] Cozar R and Pineau A 1973 *Metall. Trans.* **4** pp 47-59.

[7] Kohn W and Sham L J 1965 *Phys. Rev. A* **140** 1133.

[8] Kresse G and Furthmuller J 1996 *Phys. Rev. B* **54** pp 11169-11186.

[9] Kresse G and Joubert D 1999 *Phys. Rev. B* **59** pp 1758-1775.

[10] Ceperley D M and Alder B J 1980 *Phys. Rev. Lett*. **45** 556.

[11] Perdew J P, Burke K and Ernzerhof W 1996 *Phys. Rev. Lett.* **77** 3865.

[12] Methfessel M and Paxton A T 1989 *Phys. Rev. B* **40** pp 3616-3621

[13] Blöchl P E, Jepsen O and Andersen O K 1994 *Phys. Rev. B* **49** pp 16223-16233.

[14] Murnaghan F D 1944 *Proc. Natl. Acad. Sci.* USA **30** 244.

[15] Guo G, Wang Y and Hsu LS 2002 *J MagnMagn Mater* **239** 91.

[16] Kim D, Shang S and Liu Z 2010 *Intermetallics* **18** 1163.

[17] Rao PM, Suryanarayana S, Murthy KS and Naidu SN 1989 *J Phys Condens Matter* 15357.

[18] Yasuda H, Takasugi T and Koiwa M 1992 *ActaMetall Mater* **40** 381.

[19] Lin Y C, Luo S, Chen M, He D and Zhao C 2016 *J. Alloys Compd.* **688** pp 285-293.

[20] Connetable D, Mathon M and Lacaze J 2011 *Coupling Phase Diagrams Thermochem* **35** pp 588-593.

[21] Duan Y H, Hu W C, Sun Y and Peng M J 2014 *J. Alloys Compd.* **614** pp 334-344.

[22] Kim D E, Shang S L and Liu Z K 2010 *Intermetallics* **18** pp 1163-1171.

[23] Wu Q and Li S 2012 *Comput. Mater. Sci.* **53** pp 436-443.

[24] Sundararaman M, Mukhopadhyay P and Banerjee P 1988 *Metall. Trans.* **19A (3)** 453.

[25] Hamid A S, Uedono A, Major Z, Haynes T D, Laverock J, Alam M A, Dugdale S B, and Fort D 2011 *Phys. Rev. B* **84** 235107.